# Temperature Controls the Lifetimes and Microbial Communities Degrading Cellulose Diacetate in the Coastal Ocean

Yanchen Sun[†]*, Bryan D. James[#], Katelyn R Houston[▽], Brian Edwards[▽], Mounir Izallalen[▽], Sharmistha Mazumder[▽], Rahul Shankar[▽], Christopher M. Reddy[†], and Collin P. Ward[†]*

[†]Department of Marine Chemistry and Geochemistry, Woods Hole Oceanographic Institution, Woods Hole, Massachusetts 02543, United States

[#]Department of Chemical Engineering, Northeastern University, Boston, Massachusetts 02115, United States

[▽]Eastman, Kingsport, Tennessee 37662, United States

***Corresponding authors:**

Yanchen Sun, Department of Marine Chemistry and Geochemistry, Woods Hole Oceanographic Institution, 266 Woods Hole Road, Woods Hole, Massachusetts 02543, United States, Phone: +1 865-309-3246, Email: yanchen.sun@whoi.edu

Collin P. Ward, Department of Marine Chemistry and Geochemistry, Woods Hole Oceanographic Institution, 266 Woods Hole Road, Woods Hole, Massachusetts 02543, United States, Phone: +1 508-289-2931, Email: cward@whoi.edu

## Abstract

Cellulose diacetate (CDA), a bio-based material widely used in consumer products, is biodegradable in the coastal ocean. However, the effect of water temperature on biodegradation rates is unknown, limiting projections of lifetime across space and time. Here, we incubated CDA-based materials (film, foam, and straw), paper straws, polyethylene (PE) films, and polybutylene adipate terephthalate (PBAT) straws for 28 weeks at 10 and 20 °C in continuous-flow seawater mesocosms. The relative mass loss of the CDA film, foam, and straw increased by 20–25% from 10 to 20 ºC, and their degradation rates increased by 1.8- to 3.1-fold. Accordingly, model predictions of CDA-based article lifetimes in North American coastal waters were highly sensitive to differences in water temperature across latitude and seasonality. Paper straws also showed a notable temperature dependence, with degradation rates increasing 1.7-fold from 10 to 20 °C. PE films and PBAT straws showed no measurable degradation at either temperature, highlighting their persistence in the environment. Microbial communities implicated in CDA biodegradation were influenced by material type, temperature, and incubation time. Differential analysis revealed that ~93% (29/31) of the highly responsive microbial taxa implicated in the degradation of CDA were unique at 10 and 20 °C. These findings indicate that water temperature governs the lifetime of biodegradable materials, supporting its inclusion as a primary variable in experimental frameworks moving forward.



**Keywords:** plastic pollution, bioplastics, marine biodegradation, temperature, microbial communities, 16S rRNA gene amplicon sequencing.


**Synopsis:** The rates and communities implicated in the degradation of cellulose diacetate-based materials in the coastal ocean are strongly mediated by seawater temperature.

46 **TOC graphic.**

47 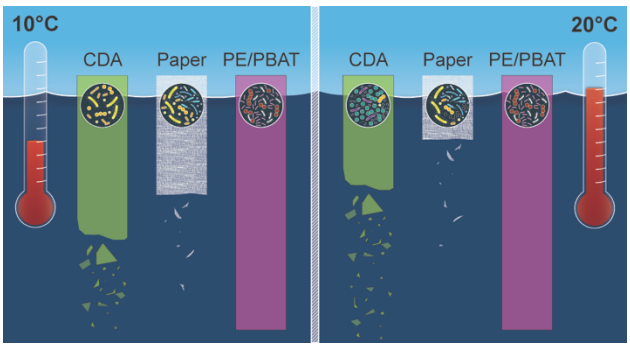

## Introduction

Plastics in the marine environment are a major concern due to their high volume, environmental persistence, and potential threats to wildlife and humans.[1-4] Notably, most plastics are derived from fossil hydrocarbons and have lifetimes of decades to centuries.[2, 5-7] A promising solution to limit plastic pollution is to replace fossil carbon-based conventional plastics with sustainably sourced, high-functioning, and low-persistence bioplastics.[8-10]

Cellulose diacetate (CDA) is a bio-based material that has been widely used in consumer goods, including drinking straws,[7] textiles,[11] and cigarette filters.[12, 13] CDA can be biodegraded in natural seawater environments on time scales of months,[7, 14, 15] orders of magnitude faster than conventional plastics.[5, 7] Detailed degradation mechanisms and potential degrading microbial communities have been identified;[14, 15] however, understanding of other environmental factors (e.g., temperature) that may influence the rate and communities implicated in degradation in the coastal ocean remains limited.

Seawater temperature varies in time and space. For example, the sea surface temperatures (SSTs) typically range from 10 to 15 °C during winter and from 20 to 30 °C in summer in the mid-latitudes of the Northern Hemisphere.[16] Under current climate projections, global SSTs are expected to rise by 1–3.5 °C by the end of the 2100.[17] These variations in SSTs may affect the biodegradation of CDA because biological processes are sensitive to temperature. The $Q_{10}$ temperature coefficient for surface ocean respiration, which reflects the sensitivity of microbial metabolic rates to a 10 °C increase in temperature, typically ranges from 1.5 to 3.6;[18-20] however, the temperature sensitivity of bioplastic degradation under various thermal conditions is severely limited. CDA degradation is an enzymatically driven process in which acetyl groups are cleaved first (i.e., deacetylation) by esterases, then cellulose groups are degraded by cellulases.[14] The

enzymatic activities of esterases and cellulases are sensitive to temperature, and their optimal activity conditions further depend on the host microorganisms, suggesting that rates of degradation are likely sensitive to temerpature.[21, 22] In addition, temperature also affects the composition of the microbial community in seawater, with psychrophiles dominating at ~10 °C and mesophiles dominating at 20-45 °C.[23, 24] Changes in the microbial community may, therefore, affect its metabolic potential. Hence, understanding the kinetics and functional microbial communities that underlie CDA biodegradation under different temperature conditions could advance our understanding of the fate of CDA pollution in the coastal ocean.

The objectives of this study were to examine how temperature affects the degradation of CDA bioplastics in the coastal ocean, model the lifetime of CDA bioplastics across space and time, and identify specific microorganisms that may drive biodegradation as a function of temperature. To achieve these objectives, we incubated CDA films, foams, and straws in continuous-flow mesocosms with natural seawater alongside materials with high degradability (paper straw),[7] and low degradability (polyethylene [PE] film and polybutylene adipate terephthalate [PBAT] straw).[14, 25] Degradation experiments were conducted at 10 and 20 °C, bracketing the global average sea surface temperature of 16 °C.[16, 26] We assessed the biodegradation of these materials by measuring the mass loss across 28 weeks of incubation, determined the relationship between degradation rates and seawater temperature, and modeled the lifetime of CDA bioplastics in North American coastal waters across latitudinal gradients and seasonality. We also characterized the microbial communities associated with these materials, affording new knowledge of how communities vary with temperature, time, material type, and morphology.

## Materials and Methods

**Materials.** CDA film (thickness = 113 μm, $\rho_{solid}$ = 1.35 g $cm^{-3}$), foam (3,750 μm, $\rho_{low}$ = 0.12 g $cm^{-3}$), and straw (175 μm, $\rho_{solid}$ = 1.35 g $cm^{-3}$) were obtained from Eastman (Kingsport, TN, USA). Paper straw (376 μm) was purchased from Amazon (Harvestraw). PE film (25 μm) was purchased from Unifi Manufacturing Inc. (Greensboro, NC, USA). PBAT straw (269 μm) was bought from Vegware (Boulder, CO, USA). The PBAT straw is composed of 85% PBAT and 15% polylactic acid (PLA) by weight (hereafter referred to as PBAT straw) and it meets compostable standards (ASTM D6400 and EN13432). Among these six materials, only three CDA materials contain approximately 15–20 wt% of a biodegradable plasticizer (i.e., triacetin), which has been shown to leach quickly into seawater.[7, 14, 27]

**Incubation of CDA bioplastics and control materials in the seawater mesocosm.** CDA and control materials were incubated in continuous flow-through seawater mesocosms with filtered natural seawater.[14] The plastic materials with low degradability, PE film and PBAT straw were used as the negative control,[14, 28] and the paper straw with a high degradability was selected as the positive control.[7] Straw materials, each 25.4 mm in length, and all other materials, cut to 25.4 × 25.4 mm (length × width), were incubated in the mesocosm using stainless steel wire holders for the straws and clamps for the films and foams. Detailed information on the mesocosm setup (Figure S1) and seawater has been described previously.[14] Seawater with a salinity of ~30 ppt[29] containing native microbial communities was drawn from Martha's Vineyard Sound (Woods Hole, MA, USA) and filtered using a 200 μm filter for removing larger particles. Pre-tempered (10 and 20 °C) was deposited into head tanks, providing an equal flow rate of approximately 0.7 L $hour^{-1}$ with a residence time of ~1-h in the mesocosm with a size of 54 × 34 × 25cm (length × width × height). Degradation experiments were performed at 10 and 20 °C in the absence of sunlight (Figure S1). The temperature was monitored throughout the experiment, averaging 10.4

± 0.7 °C and 20.2 ± 0.6 °C, respectively. A total of 252 samples were incubated throughout the experiment.

**Sample collection and mass loss measurements.** To record photographic evidence of degradation and assess mass loss, samples were collected across 28 weeks of incubation. Briefly, each sample was photographed and then transferred into a pre-weighed 2 mL microcentrifuge tube. Biofilms were removed by incubating each sample for ~30 min at room temperature and then rinsed with copious amounts of Milli-Q water.[14] Subsequently, the samples in their respective tubes were dried at 60 °C for 48 hours in an IsoTemp 637G oven (Fisher Scientific). The samples were removed from the oven and cooled to room temperature before being weighed. Three replicates were collected for each material type at each sampling time point and temperature condition.

Mass loss was calculated as the relative mass loss (%) by taking the difference between the initial mass of the sample ($m_0$) and the mass of the sample at a time point ($m_t$), then normalizing it to the initial mass of the sample (Eq 1). Mass loss measurements of CDA materials were reproducible and repeatable over multiple years and seasons.[7, 14, 27] Mass loss is a reasonable measure for the degradation of CDA and paper materials because it is well-established that these materials biodegrade to $CO_2$ in the coastal ocean.[7, 14] Previous experiments have determined that no mass loss occurred in sterilized controls.[15]

$$Mass\ loss\ (\%) = \frac{m_0 - m_t}{m_0} \times 100\% \qquad \text{(Eq 1)}$$

**Surface erosion model.** Since degradation occurs principally at exposed surfaces, we assume the degradation rate to be proportional to the surface area. The relative mass loss data was fit to a phenomenological surface erosion model (Eq 2) in which $\partial m/\partial t$ is the change in mass with time,

139 $m$ is the instantaneous mass, $k_d$ is the specific surface degradation rate, $A_s$ is the surface area, and
140 $V$ is the volume.[30, 31]

141 $$\frac{\partial m}{\partial t} = -mk_d \frac{A_s}{V} \quad \text{(Eq 2)}$$

142 Eq 2 was applied to a material of initial length $l_0$, width $w_0$, and thickness $h_0$, and then adjusted
143 using a constant $\beta$ to account for mass loss due to leachable components (e.g., plasticizer) or other
144 initial mass changes between the initial mass and the first time point. This adjustment resulted in
145 Eq 3 for film and foam and Eq 4 for straw. As a result, the trivial data point representing zero mass
146 loss at time zero was excluded from the model fitting.

147 $$Mass\ loss\ (\%) = 100\% \times \left[\left(1 - \frac{(l_0-2k_dt)(w_0-2k_dt)(h_0-2k_dt)}{l_0w_0h_0}\right)(1-\beta)+\beta\right] \quad \text{(Eq 3)}$$

148 $$Mass\ loss\ (\%) = 100\% \times \left[\left(1 - \frac{(l_0-2k_dt)(h_0-2k_dt)}{l_0h_0}\right)(1-\beta)+\beta\right] \quad \text{(Eq 4)}$$

149 $l_0$ and $w_0$ were assumed to be 25.4 mm for each sample, which is valid because Eqs 3 and 4 are
150 largely insensitive to changes in $l_0$ and $w_0$ when $l_0 \gg h_0$ and $w_0 \gg h_0$ as is the case for the film,
151 foam, and straw samples.

152 **Regression analyses.** The relative mass loss data was fitted to Eq 3 or Eq 4 using nonlinear
153 least-squares regression. Relative mass loss data for PE film and PBAT straw were not fitted
154 because any mass loss was within the uncertainty of the mass loss measurements. Instead, mass
155 loss trajectories were constrained for these materials using specified values of $k_d$ and the sample's
156 dimensions. All regressions were performed in R (version 4.0.2).[32] Projected environmental
157 lifetimes ($t_L$) were calculated using Eq 5.

158 $$t_L = \frac{h_0}{2k_d} \quad \text{(Eq 5)}$$

159 **CDA bioplastic lifetime projections.** The degradation rates of bioplastics in natural
160 environmental systems follow the Arrhenius equation.[33] The natural log transformation of the

Arrhenius equation is shown in (Eq 6), where $E_a$ is the activation energy of the degradation, $R$ is the gas constant, $T$ is the temperature, and $A$ is the pre-exponential factor. Because the lifetime of CDA bioplastic is dependent on its thickness ($h_0$) and the specific surface degradation rate ($k_d$) (Eq 5), we formulated Eq 6 by incorporating Eq 5 and obtained the relationship between lifetime and temperature (Eq 7).

$$lnk_d = -\frac{E_a}{RT} + lnA \quad \text{(Eq 6)}$$

$$t_L = \frac{h_0}{2A} e^{\frac{E_a}{RT}} \quad \text{(Eq 7)}$$

This relationship (Eq 7) makes it possible to predict the persistence of CDA bioplastics in the broader natural marine environment. Briefly, the lifetimes of CDA bioplastics in coastal oceans were projected by transforming 1° × 1° gridded maps of SSTs generated by CMIP multi-model means by applying Eq 7. We used modeled historical SSTs from 1995–2014 to represent current ocean conditions, with winter SSTs and summer SSTs corresponding to the annual minimum and maximum temperatures, respectively. Models of future winter and summer SSTs from 2081–2100 were used to represent the projected annual minimum and maximum temperature conditions, respectively. SST models were available from the IPCC WGI Interactive Atlas (https://interactive-atlas.ipcc.ch/). The projections were performed in R with packages rnaturalearth,[34] terra,[35] and tidyterra.[36]

**DNA extraction, 16S rRNA gene amplification, and sequencing.** For time series collection, three biological replicates per material per temperature condition were collected from the biodegradation experiment (see above) at week 4 and 28, respectively. Seawater samples were also collected for comparison by filtering 1 L of seawater from the mesocosm using 0.2 μm sterilized PES filters (Nalgene, Rochester, NY, USA) at identical two sampling time points. Four seawater samples were collected at two-time points under two temperature conditions, each containing three

184 biological replicates. Seventy-two biofilm and 12 seawater communities were sequenced for each
185 material type throughout the experiment. All samples were stored at -20 °C before DNA extraction.
186 The entire sample was subjected to DNA extraction using the DNeasy PowerBiofilm kit (Qiagen,
187 Hilden, DE) according to the manufacturer's instructions, and concentrations were determined
188 using the Qubit High Sensitivity dsDNA assay (Life Technologies, Carlsbad, CA, USA).
189 Amplicon libraries for variable region V3-V4 were prepared following previously established
190 procedures.[7, 37] The pooled amplicon libraries were sequenced using a 2 × 300 bp MiSeq platform
191 (Illumina) at the Institute for Genome Sciences at the University of Maryland. Amplicon reads
192 were processed using the QIIME2 pipeline[38] for quality control, merging sequences, and assigning
193 amplicon sequence variants (ASVs). Taxonomy was assigned against the SILVA v138 (silva-138-
194 99-nb-classifier.qza) database.[39, 40] No amplification was detected in any of the negative PCR
195 controls, and the one representative PCR negative control that was sequenced had a minimal
196 number of sequences that did not pass the quality filtering and denoising steps. The 16S rRNA
197 gene amplicon sequencing data generated in this study were deposited in the European Nucleotide
198 Archive under project PRJNA1210484, and their respective accession numbers can be found in
199 Table S1.
200 **Statistical analyses.** Statistical analyses and plotting were performed in R (4.0.2). Beta-
201 diversity was calculated using Bray–Curtis dissimilarity and visualized using the principal
202 coordinate analysis (PCoA) plot in R with packages ggplot2[41] and phyloseq[42]. Statistical
203 differences in microbial communities among different materials and incubation times were
204 determined using permutational multivariate analysis of variance (PERMANOVA) in R with
205 package vegan.[43] Identifying potential microbial taxa implicated in CDA degradation under
206 different temperature conditions was conducted following a previously established procedure.[15]

Briefly, the differential analysis of the relative microbial abundances between CDA and cellulose-based positive material of the same morphology (i.e., straw) was conducted using the DESeq2[44] and the data was visualized using ggplot2.[41] It has been demonstrated that CDA degradation is a two-step process comprising the deacetylation and degradation of cellulose groups.[14] Accordingly, the differential microbial communities between CDA material and the positive control represent the potential CDA-degrading microbial groups.

## Results and Discussion

**CDA degradation under different temperature conditions.** Photographic evidence indicated biofouling communities formed on the surface of the CDA and control materials within weeks under the 10 and 20 °C conditions (Figure 1). The extent of biofouling increased over time for all materials. Mass loss measurements demonstrated substantial sensitivity to seawater temperature for those materials that degraded. At 10 °C, the CDA film, foam, and straw lost 35 ± 7, 23 ± 1, and 32 ± 2% of their initial mass after 28 weeks of incubation, respectively. In contrast, more than 55 ± 5, 48 ± 6, and 57 ± 2% of their initial mass was lost for CDA film, foam, and straw at 20 °C during the same incubation period. For the three CDA bioplastics, the rapid mass loss in the first 3.5 weeks was due to the release of the biodegradable plasticizer, triacetin, which exhibited similar leaching rates under both temperature conditions. The subsequent mass loss reflects the degradation of the CDA polymer. The mass loss of the paper straw was also sensitive to temperature, with 43 ± 1% mass loss at 10 °C and 71 ± 5% at 20 °C.

The significant impact of temperature on CDA biodegradation rates was likely driven by the temperature sensitivity of the enzymes responsible for CDA degradation. Specifically, the activities of esterases and cellulases, two key enzymes that drive CDA degradation, were expected

to be temperature-sensitive. Research efforts have shown that the optimal temperatures for salt-tolerant esterases and cellulases are typically above 20 °C [45-48]. Consistently, degradation of CDA bioplastics was more rapid at 20 °C than at 10 °C.

Compared to CDA and paper, the PE film and PBAT straw did not degrade at either temperature (Figure 1). While PE was expected to be persistent,[14] evidence to date on the fate of PBAT in the ocean is limited. Although PBAT bioplastics have been reported to degrade in composting systems,[49] soils,[50] and freshwater environments,[51] an increasing number of studies highlight its persistence in the ocean,[28, 52-54] including our study (Figure 1). These findings underscore the need to assess degradation in diverse environments prior to universally classifying a polymer as "biodegradable." Alternatively, studies could prioritize testing of degradation in more challenging environments (e.g., the ocean) and then reasonably assume degradation in more nutrient-rich, productive environments (e.g., freshwater or composting), simplifying the experimental matrix and reducing costs to manufacturers.

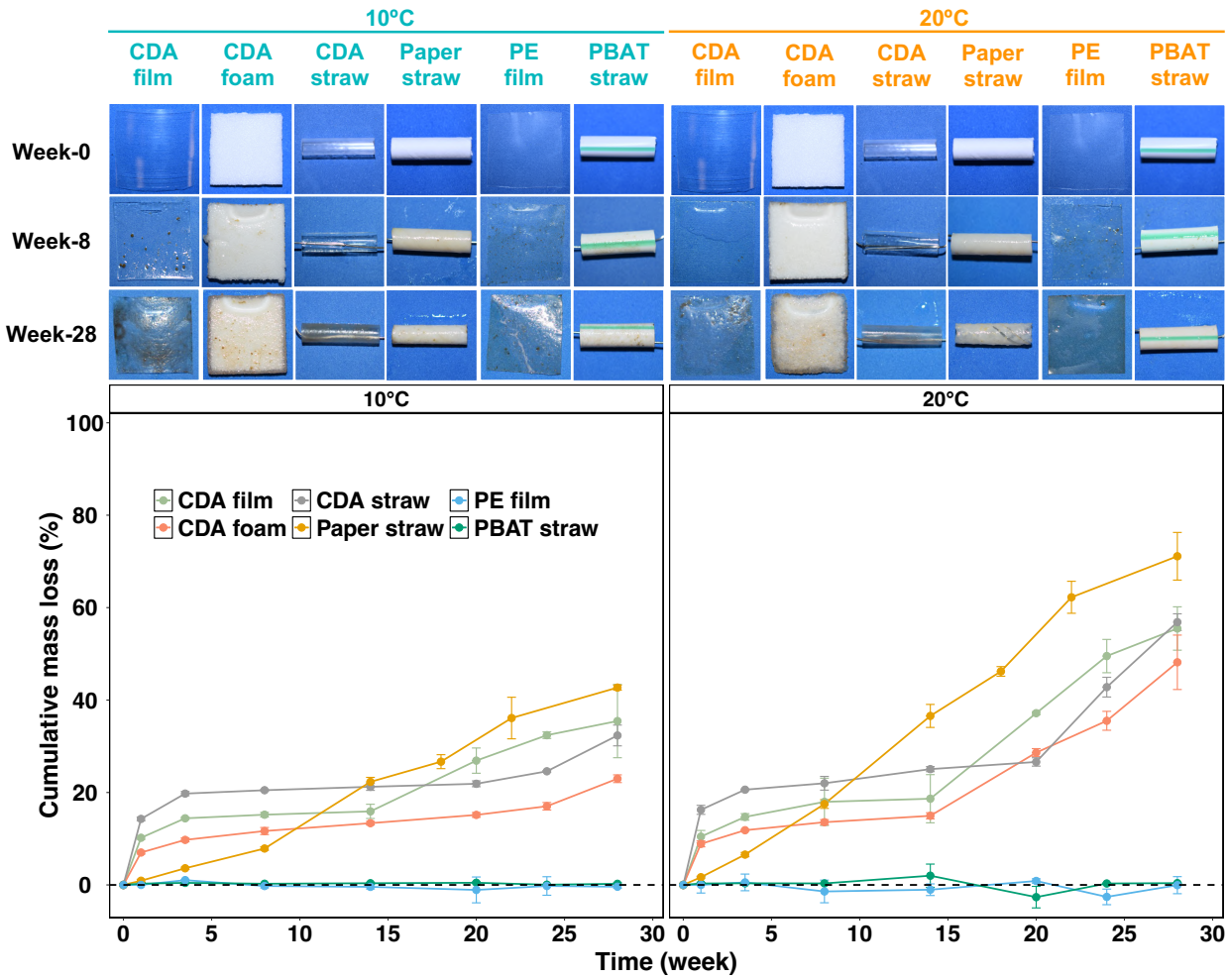


**Figure 1.** Degradation of CDA bioplastics under 10 and 20 °C conditions in natural seawater. (Upper panel) Time-lapse photography of CDA, paper, PE, and PBAT materials over a 28-week incubation in the continuous-flow seawater mesocosm. (Lower panel) Cumulative mass loss of six different materials over a 28-week incubation period in the continuous-flow seawater mesocosm. Error bars represent the standard deviation of three replicate materials and are not visible when smaller than the symbol size.

**The lifetime of CDA bioplastics depends on seawater temperature.** The biodegradation of CDA materials is a surface-driven process,[30, 31] so the lifetime of CDA materials depends on their thickness and specific surface degradation rate (Eqs 3 and 4, see the Methods for details, Figure

S2). The $k_d$ values for CDA film, foam, and straw at 10 °C were 30 ± 3, 388 ± 36, and 22 ± 3 μm year$^{-1}$, respectively (Figures 2 and S3, Table S2). However, the $k_d$ values for CDA film, foam, and straw at 20 °C were 54 ± 4, 1,207 ± 104, and 68 ± 7 μm year$^{-1}$, respectively, which were approximately 80%, 211%, and 207% higher than those at 10 °C, respectively. The $k_d$ value for paper straw at 10°C was 160 ± 6 μm year$^{-1}$, which increased to 259 ± 5 μm year$^{-1}$ at 20 °C. Based on calculated mass loss trajectories, the $k_d$ values for PE film and PBAT straw were constrained to less than 2 μm year$^{-1}$.

Across all CDA and paper materials tested, $Q_{10}$ values, or the increase in degradation rate with a 10°C increase in temperature, ranged from 1.6 to 3.1. These values fall within the range of $Q_{10}$ values of 1.5 to 3.6 for pelagic microbial rate processes (e.g., respiration and bacterial productivity),[18-20] suggesting that CDA and paper materials exhibit temperature sensitivities comparable to those of natural marine microbial processes.

The environmental lifetimes for the CDA and control materials were projected using the $k_d$ values and the thickness of each material (Table S2). The projected environmental lifetimes of the CDA film (113 μm), foam (3,750 μm), and straw (175 μm) at 10 °C were 1.9 ± 0.1, 4.8 ± 0.1, and 3.9 ± 0.2 years, respectively. The projected environmental lifetimes of these three CDA materials at 20 °C were significantly shorter, being 1.0 ± 0.05, 1.6 ± 0.02, and 1.3 ± 0.05 years, respectively. The lifetimes of the paper straw in the coastal ocean at 10 and 20 °C were 1.2 ± 0.03 and 0.7 ± 0.02 years, respectively.

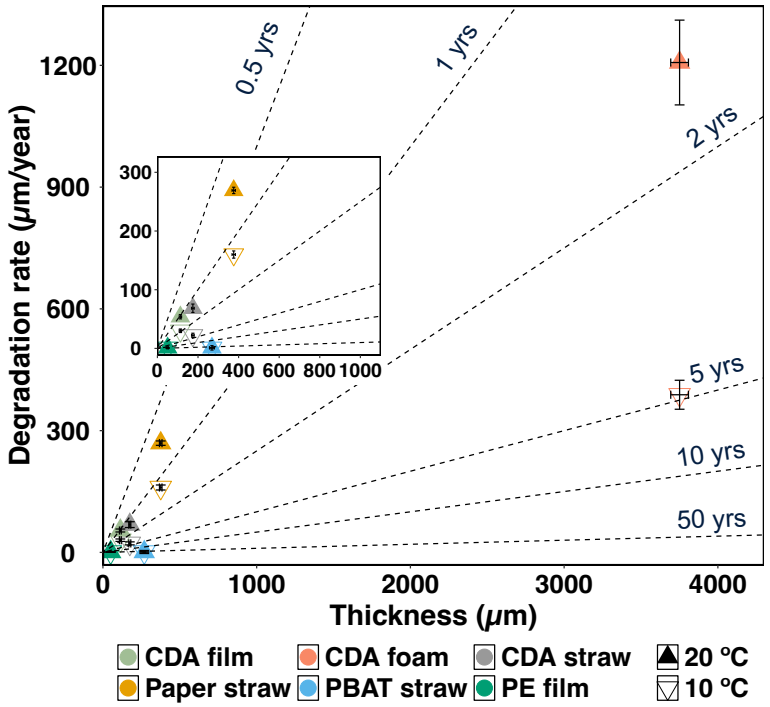


**Figure 2.** Projected lifetimes of the CDA materials and paper straw under 10 and 20 °C conditions in natural seawater. Lifetime depends on material functional properties (i.e., thickness; x-axis) and degradation properties (i.e., $k_d$; y-axis). Data points represent mean ± standard deviation in the horizontal and vertical directions. Dashed lines indicate iso-lines of the projected environmental lifetime based on eq 4 described in the methods. The insets present the projected lifetime of six tested materials with a thickness of less than 1000 μm.

Provided the measured $k_d$ at 10 and 20 °C and assuming that the biodegradation rates of the plastics follow the Arrhenius equation,[33] modeled predictions of the lifetime of CDA foam were computed across time and space in the North American coastal ocean (Figures 3 and S5). As expected, the lifetime of CDA foam in high-latitude coastal waters is significantly longer than in low-latitude areas, irrespective of seasonality changes (Figure 3). Additionally, the projected lifetime of CDA foam was more sensitive to seasonal SST changes, particularly in middle-latitude

regions. The $\Delta CDA_{lifetime}$ between 26° and 60° latitude on the west coast and between 28° and 50° latitude on the east coast is longer in winter (minimum temperature condition) than in summer (maximum temperature condition). For example, the projected lifetime of CDA foam with a thickness of 3,750 µm in Cape Cod Bay, MA, USA (69.5°W, 42.5°N) is approximately 6.3 years in winter (minimum condition of 7.7 °C) and 2.0 years in summer (maximum condition of 17.8 °C) (Table S3).

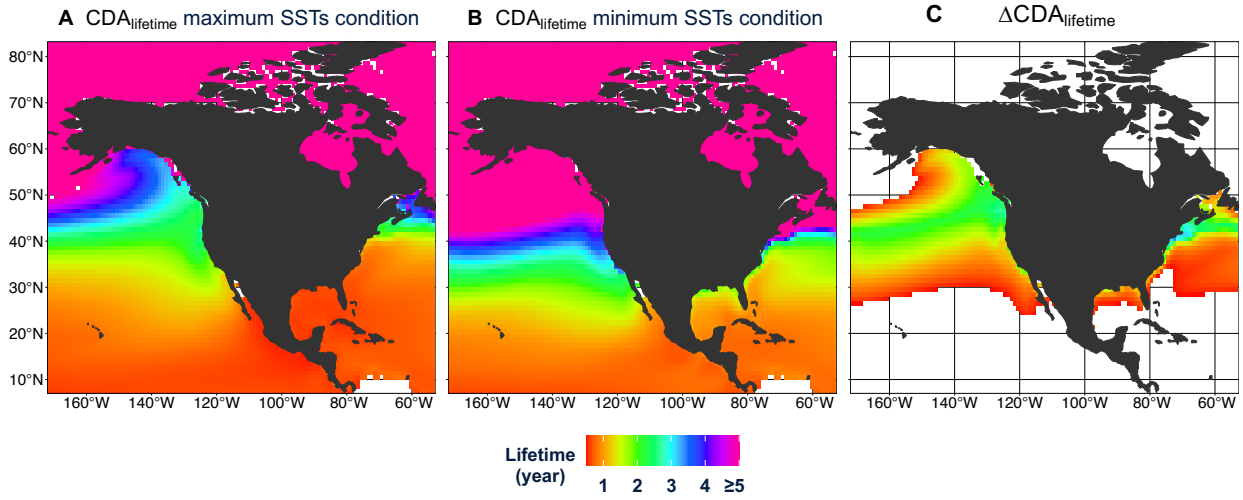


**Figure 3.** Current projections of the CDA foam lifetime based on sea surface water temperature under the Sustainable Development (SSP1-2.6) scenario. (A) Current CDA foam lifetime in the mixed layer predicted using the CMIP6 multimodel mean summer sea surface temperature (June to August, 1995–2014) under maximum temperature conditions. (B) Current CDA foam lifetime in the mixed layer predicted using the CMIP6 multimodel mean winter sea surface temperature (December to February, 1995–2014) under minimum temperature conditions. (C) Change in absolute CDA foam lifetime (ΔCDAlife) of the current projection using SSTs under the SSP1-2.6 scenario in the same models (1995–2014). A CDA foam lifetime equal to or longer than 5 years is represented in pink.

Under current climate projections, global SSTs are expected to rise by 1–3.5 °C by the end of the 2100.[17] Elevated temperatures have been shown to accelerate plastic degradation.[33, 55] To assess how the environmental persistence of CDA foam shifts under future warming conditions, we computed CDA foam lifetimes using end-of-century SST conditions (2081-2100, Figure S5). The projected lifetime of CDA foam is shorter in low- and middle-latitude regions under future warming conditions than that of the present. For example, the projected SSTs in Cape Cod Bay at the end of 2100 are about 2 °C higher than present in winter and summer. Accordingly, the projected lifetime of CDA foam in the same area of Cape Cod Bay is approximately 1.6 years under maximum temperature conditions and 5.9 years under minimum temperature conditions (Table S3), both of which are slightly shorter than the lifetimes under present temperature conditions. Collectively, seasonal temperature changes have a far more pronounced effect on the lifetime of a biodegradable material than the future warming of SST.

**Microbial community composition.** Principal coordinate analysis showed that the clustering patterns of microbial communities in various materials were mainly determined by material type, incubation time, and temperature ($P < 0.01$, PERMANOVA) (Figure S6 and Table S5). Specifically, the CDA materials had unique microbial communities based on morphology (i.e., film, foam, and straw), and the communities shifted significantly with temperature and time (Figures 4 and S6), suggesting that the microorganisms that degrade these materials were selected. In contrast, the communities grown on PE film were separate from those on the CDA materials, positive control, and seawater. Still, they remained relatively stable under different temperatures and incubation times (Figure S6). The communities grown on the PBAT straw were temperature sensitive at week-4, but were similar at week-28 irrespective of temperature conditions.

Additionally, the PE film and PBAT straw had similar community structures at week-28 despite the different materials and temperatures. This result suggests that non-degradable materials only provide surfaces for the colonization of microorganisms rather than substrates for metabolism. Communities from the paper straw differed from the other samples ($p < 0.01$, PERMANOVA). Still, they remained stable across 28 weeks of incubation at 10 and 20 °C ($p > 0.05$, PERMANOVA), suggesting that the same group of microorganisms was responsible for cellulose degradation. The microbial communities in the seawater remained relatively stable over the 28-week incubation period at both temperatures.

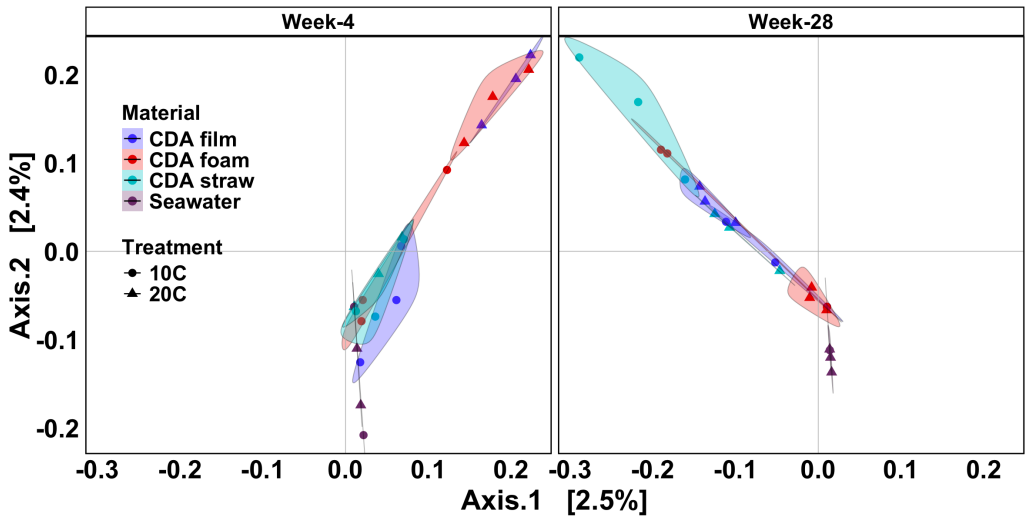


**Figure 4.** Beta diversity of microbial communities based on Bray–Curtis dissimilarity of 16S rRNA gene sequences. Samples are visualized by principal coordinates analysis.

Differential abundance analysis revealed significant differences in microbial communities inhabiting CDA film, foam, and straw under two temperature conditions (Figures 4 and S7). For instance, at week-4, when comparing the microbial community composition of CDA films at 10 and 20 °C, we observed that 29 genera were significantly more abundant in the CDA

344 films at 10 °C. In comparison, 15 genera were more abundant at 20 °C (log2fold change > 5
345 and $p < 0.001$, Figure S8A). Of these 29 genera in CDA films at 10 °C, three genera,
346 *Neptuniibacter*, *Colwellia*, and *SM1A02*, were among the top 20 most abundant genera,
347 collectively accounting for up to 7% of the total relative abundance (Figure S7). In contrast,
348 among these 15 genera in CDA films at 20 °C, the combined relative abundance of the four
349 dominant genera, *Sva0996_marine_group*, *Winogradskyella*, *Agaribacterium*, and
350 *Sphingorhabdus*, was as high as 20% (Figures S7). For CDA foams at week-4, 20 genera were
351 significantly more abundant at 10 °C, whereas 19 genera were more abundant at 20 °C
352 (log2fold change > 5 and $p < 0.001$, Figure S8B). The most dominant genus, *Neptuniibacter*,
353 had a relative abundance of up to 4.3% at 10 °C (Figure S7). The three most abundant genera
354 of these 19 genera at 20 °C, *Sva0996_marine_group*, *Winogradskyella*, *Agaribacterium*, had
355 a total relative abundance of 12%. For CDA straws at week-4, 16 genera were more abundant
356 at 10 °C, while 21 genera were more abundant at 20 °C (log2fold change > 5 and $p < 0.001$,
357 Figure S8C). Of these 16 genera in CDA straws at 10 °C, three genera, *Neptuniibacter*,
358 *Colwellia*, and *Ulvibacter*, were among the top 20 most abundant genera with a total relative
359 abundance of up to 8.8% (Figure S7). Among the 21 genera in CDA straws at 20 °C, the
360 combined relative abundance of the three most dominant genera, *Agaribacterium*,
361 *Pelagicoccus*, and *Winogradskyella*, was as high as 5.3% (Figures S7). Overall, the structure
362 of microbial communities associated with CDA materials was significantly influenced by both
363 material type and temperature.

364 **Potential CDA-degrading microbial communities.** The biodegradation of CDA is a two-
365 step process: deacetylation of the acetyl group followed by degradation of the cellulose
366 backbone.[14] The former step, deacetylation, is the rate-limiting step,[14, 15, 56] and thus,

367 microorganisms that initiate deacetylation are key drivers of CDA degradation. Accordingly,
368 differential abundance analysis of the community composition between a CDA material and
369 a cellulose-based positive control of the same morphology (i.e., straw) may thus reveal
370 microbial communities that drive the deacetylation of CDA (Figure 5).

371 Differential abundance analysis revealed that 20 highly responsive ASVs were
372 significantly increased in relative abundance in CDA straw compared to paper straw at 10 °C
373 at week-4, with log2fold changes ranging from +7 to +11 and $p < 0.001$ (Figure 5A). The
374 average relative abundance of these ASVs in CDA straw samples ranged from 0.1 to 2.9%
375 (Figure S9). At 20 °C, 11 ASVs were identified as markedly increased in the relative
376 abundance in CDA straw compared to paper straw (Figure 5B). The average relative
377 abundance of these 11 ASVs in CDA straw samples ranged from 0.6 to 5.2%. Genus-level
378 microbial community composition analysis of these highly responsive ASVs from CDA
379 straws at 10 and 20 °C revealed temperature dependence. Only two ASVs affiliated with the
380 genera *g_Candidatus_Kaiserbacteria* and *g_Eudoraea* were identified in CDA straws under
381 both temperature conditions, and the rest of the ASVs were unique (Figures 5 and S9). These
382 findings suggest that temperature selects for unique microbial communities that metabolize
383 CDA.

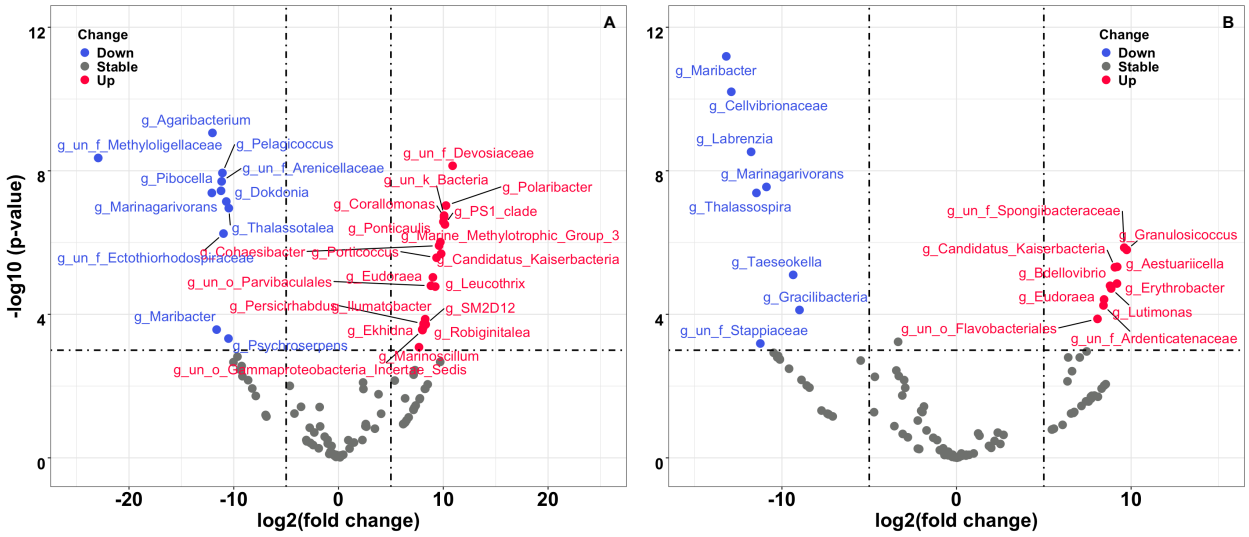


**Figure 5.** Microbial communities exhibited significant changes in relative abundance between CDA straw and paper straw at 10 °C (A) and 20 °C (B) at week-4. Three biological replicates derived from the same type of material were pooled together. The communities with an adjusted $p < 0.001$ and log2fold change > 5 were considered significantly different. Taxa shown in blue and red represent communities in the CDA straw treatment that significantly decreased and increased in relative abundance compared to the corresponding paper straw control, respectively. ASVs shown in gray indicate no significant change in relative abundance of communities between CDA straw and paper straw per temperature condition. The taxonomy of these significantly changed communities was assigned to a genus, or the lowest level can be assigned.

Regardless of morphology (e.g., film, foam, and straw), CDA materials were efficiently degraded at both 10 and 20 °C, and biodegradation was driven by different marine communities (e.g., film, foam, and straw) (Figures 4, S7, and S8). These findings suggest that temperature exerts selection on microbial communities, and further support that temperature affects biological processes by determining community composition.[23, 24] Most taxa that exhibited a significant

increase in relative abundance at 10 °C compared with 20 °C (e.g., *Neptuniibacter*, *Colwellia*, *SM1A02,* and *Ulvibacter*) have been previously found in cold marine environments.[57-60] In contrast, taxa that dominated at 20 °C (e.g., *Sva0996_marine_group*, *Winogradskyella*, *Agaribacterium*, *Pelagicoccus*, and *Sphingorhabdus*) were frequently detected in mesophilic marine environments.[61-64] These findings emphasize that temperature affects the degradation of CDA bioplastics by selecting distinct microbial communities, highlighting the importance of incorporating temperature into the assessment of marine biodegradation of materials.

**Comparing the relative importance of temperature to surface area on material degradation rates.** While the findings of this study highlight the sensitivity of CDA biodegradation rates to water temperature, this environmental control is relatively less important than surface area, a material property control. The current study demonstrates that the degradation rate of CDA foam increased by 3.1-fold when the temperature rose from 10 to 20 °C (Figures 2 and S3). Using the same experimental system and material, we recently reported that when switching from solid CDA to low-density CDA foam, the degradation rate at 20 °C increased by approximately 15-fold (Figure S10).[7, 14, 27] Therefore, altering the material properties to increase surface area exerts a disproportionate impact on the persistence of CDA in the coastal ocean compared to water temperature. This result suggests that future material designs aimed at reducing the environmental persistence of biodegradable materials, especially in colder waters, should prioritize the development of material-efficient articles with increased surface area.[7, 14, 27]

**Implications for improved environmental relevance of standardized testing.** Given the notable role of temperature driving both the rates and microbial communities implicated in CDA degradation in the coastal ocean, our findings strongly advocate for incorporating temperature as an experimental variable in assessment matrices and adopting open- versus closed-system

424 incubations. Current standard methods for assessing plastic degradation in marine environments
425 are typically performed at temperature (i.e., 30 °C) within the mesophilic range using closed-
426 systems (i.e., bottles) to assess degradation over time.[52, 65] For instance, ASTM D6691 and ISO
427 22403 outline standard test methods that evaluate the biodegradation of plastics by marine
428 microorganisms at 30 °C in bottle incubations. Because 30 °C is nearly twice the global average
429 sea surface temperature of 16 °C,[16, 26] and biodegradation is highly sensitive to water temperature
430 (Figure 1), the rates determined in standard method incubations are likely artificially high.[33, 66]
431 This discrepancy raises questions about the applicability of the timelines determined using
432 standard methods to what happens in natural waters.

433 Furthermore, because the standard test methods in marine environments are optimized for
434 activating mesophilic microorganisms,[52, 65] and the communities driving degradation are sensitive
435 to temperature (Figures 4, 5, S6, and S8), the standard conditions are not directly translatable to
436 cooler, mid- and high-latitude waters where both psychrophilic and/or mesophilic microorganisms
437 dominate.[23, 24] In such regions, the rate of degradation likely vary with the source of the seawater
438 due to the different metabolic activities of psychrophilic and mesophilic microbial communities.
439 The limited translation is amplified when using closed-system (e.g., bottle) incubations, as
440 prescribed by standard tests. In bottle incubations, natural microbial communities and nutrients are
441 not replenished over time, likely hindering the evolution of the material degrading consortium
442 throughout the months-long incubation. In contrast, open-systems, such as the flow-through
443 mesocosm approach taken in the current study, ensure that microbial communities and nutrients
444 are continuously replenished, thereby better reflecting what happens in nature. To improve the
445 accuracy of material degradation predictions and to better understand the long-term persistence of
446 marine debris across space and time, we propose that future assessment matrices account for the

temperature-dependent variability in degradation rates and microbial activity, and adopt open-system incubations.

**Acknowledgments**

This work was supported by an award to CPW and CMR from the Eastman and The Seaver Institute. The authors are grateful to Rick Galat (WHOI) and the facilities team that maintains the WHOI Environmental Systems Laboratory, Amy Apprill (WHOI), Carolyn Miller (WHOI), Mallory Kastner (WHOI), and Henry Holm (Columbia University).

**Supporting Information**

The Supporting Information details CDA degradation and microbial community analysis. Table S1: 16S rRNA gene amplicon sequence information. Table S2: Results of material properties, degradation rates, and projected lifetimes. Table S3: Projected lifetime of CDA foam. Table S4: Reported degradation rates of CDA and paper materials. Table S5: Results of the PERMANOVA analysis. Figure S1: Overview of experiment setup. Figure S2: Simulation of degradation rates. Figure S3: Degradation rates comparison. Figure S4: Lifetime and temperature relationship of CDA foam. Figure S5: Future projections of CDA foam lifetime. Figure S6: Beta-diversity analysis of all samples. Figure S7: Microbial community composition at phylum, family, and genus level, respectively. Figure S8: Differential analysis for CDA bioplastics between two temperature conditions. Figure S9: Relative abundance of ASVs with markedly increased abundance in CDA straw. Figure S10: Comparison of specific surface degradation rates of CDA, paper, and conventional plastics.

## References


(1) Borrelle, S. B.; Ringma, J.; Law, K. L.; Monnahan, C. C.; Lebreton, L.; McGivern, A.; Murphy, E.; Jambeck, J.; Leonard, G. H.; Hilleary, M. A. Predicted growth in plastic waste exceeds efforts to mitigate plastic pollution. *Science* **2020**, *369* (6510), 1515-1518.

(2) Geyer, R.; Jambeck, J. R.; Law, K. L. Production, use, and fate of all plastics ever made. *Sci. Adv.* **2017**, *3* (7), e1700782.

(3) Jambeck, J. R.; Geyer, R.; Wilcox, C.; Siegler, T. R.; Perryman, M.; Andrady, A.; Narayan, R.; Law, K. L. Plastic waste inputs from land into the ocean. *Science* **2015**, *347* (6223), 768-771.

(4) Wilcox, C.; Van Sebille, E.; Hardesty, B. D. Threat of plastic pollution to seabirds is global, pervasive, and increasing. *Proc. Natl. Acad. Sci. U. S. A.* **2015**, *112* (38), 11899-11904.

(5) Ward, C. P.; Reddy, C. M. We need better data about the environmental persistence of plastic goods. *Proc. Natl. Acad. Sci. U. S. A.* **2020**, *117* (26), 14618-14621.

(6) Ward, C. P.; Armstrong, C. J.; Walsh, A. N.; Jackson, J. H.; Reddy, C. M. Sunlight converts polystyrene to carbon dioxide and dissolved organic carbon. *Environ. Sci. Technol. Lett.* **2019**, *6* (11), 669-674.

(7) James, B. D.; Sun, Y.; Izallalen, M.; Mazumder, S.; Perri, S. T.; Edwards, B.; de Wit, J.; Reddy, C. M.; Ward, C. P. Strategies to reduce the environmental lifetimes of drinking straws in the coastal ocean. *ACS Sustain. Chem. Eng.* **2024**, *12* (6), 2404-2411.

(8) Mohanty, A. K.; Vivekanandhan, S.; Pin, J.-M.; Misra, M. Composites from renewable and sustainable resources: Challenges and innovations. *Science* **2018**, *362* (6414), 536-542.

(9) Law, K. L.; Narayan, R. Reducing environmental plastic pollution by designing polymer materials for managed end-of-life. *Nat. Rev. Mater.* **2022**, *7* (2), 104-116.

(10) Zuin, V. G.; Kümmerer, K. Chemistry and materials science for a sustainable circular polymeric economy. *Nat. Rev. Mater.* **2022**, *7* (2), 76-78.

(11) Puls, J.; Wilson, S. A.; Hölter, D. Degradation of cellulose acetate-based materials: a review. *J. Polym. Environ* **2011**, *19* (1), 152-165.

(12) Araújo, M. C. B.; Costa, M. F. A critical review of the issue of cigarette butt pollution in coastal environments. *Environ. Res.* **2019**, *172*, 137-149.

(13) Ward, C. P.; Reddy, C. M.; James, B. D. Initial estimates of the lifetime of unsmoked cellulose diacetate and paper cigarette filters in the coastal ocean. *Env. sci., Adv.* **2025**.

(14) Mazzotta, M. G.; Reddy, C. M.; Ward, C. P. Rapid degradation of cellulose diacetate by marine microbes. *Environ. Sci. Technol. Lett.* **2021**, *9* (1), 37-41.

(15) Sun, Y.; Mazzotta, M. G.; Miller, C. A.; Apprill, A.; Izallalen, M.; Mazumder, S.; Perri, S. T.; Edwards, B.; Reddy, C. M.; Ward, C. P. Distinct microbial communities degrade cellulose diacetate bioplastics in the coastal ocean. *Appl. Environ. Microbiol.* **2023**, e01651-01623.

(16) Pörtner, H.-O.; Roberts, D.; Masson-Delmotte, V.; Zhai, P.; Tignor, M.; Poloczanska, E.; Mintenbeck, K.; Alegría, A.; Nicolai, M.; Weyer, N. IPCC special report on the ocean and cryosphere in a changing climate. *IPCC. Summary for Policymakers.* **2021**.

(17) IPCC. *Climate Change 2021: The Physical Science Basis.*; Cambridge Univ. Press, 2021.

(18) Robinson, C. Microbial respiration, the engine of ocean deoxygenation. *Front. Mar. Sci.* **2019**, *5*, 533.

(19) Lomas, M. W.; Glibert, P. M.; Shiah, F. K.; Smith, E. M. Microbial processes and temperature in Chesapeake Bay: current relationships and potential impacts of regional warming. *Glob. Change Biol.* **2002**, *8* (1), 51-70.

(20) Cram, J. A.; Weber, T.; Leung, S. W.; McDonnell, A. M.; Liang, J. H.; Deutsch, C. The role of particle size, ballast, temperature, and oxygen in the sinking flux to the deep sea. *Global Biogeochem. Cycles* **2018**, *32* (5), 858-876.

(21) Ferrer, M.; Chernikova, T. N.; Timmis, K. N.; Golyshin, P. N. Expression of a temperature-sensitive esterase in a novel chaperone-based *Escherichia coli* strain. *Appl. Environ. Microbiol.* **2004**, *70* (8), 4499-4504.

(22) Andreaus, J.; Azevedo, H.; Cavaco-Paulo, A. Effects of temperature on the cellulose binding ability of cellulase enzymes. *J. Mol. Catal. B Enzym.* **1999**, *7* (1-4), 233-239.

(23) Sunagawa, S.; Coelho, L. P.; Chaffron, S.; Kultima, J. R.; Labadie, K.; Salazar, G.; Djahanschiri, B.; Zeller, G.; Mende, D. R.; Alberti, A. Structure and function of the global ocean microbiome. *Science* **2015**, *348* (6237), 1261359.

(24) Deming, J. W. Psychrophiles and polar regions. *Curr Opin Microbiol* **2002**, *5* (3), 301-309.

(25) Collins, H. I.; Tabb, L.; Holohan, B. A.; Ward, J. E. Disintegration of biodegradable plastic bags in marine mesocosm conditions: the effects of time and temperature. *J. Environ. Polym. Degrad.* **2025**, *33* (2), 1035-1046.

(26) Huang, B.; Yin, X.; Menne, M.; Vose, R.; Zhang, H. NOAA global surface temperature dataset (NOAAGlobalTemp), Version 6.0 [202406], NOAA National Centers for Environmental Information. 2024.

(27) James, B. D.; Sun, Y.; Pate, K.; Shankar, R.; Izallalen, M.; Mazumder, S.; Perri, S. T.; Houston, K. R.; Edwards, B.; de Wit, J. Foaming enables material-efficient bioplastic products with minimal persistence. *ACS Sustain. Chem. Eng.* **2024**, *12* (43), 16030-16040.

(28) Delacuvellerie, A.; Brusselman, A.; Cyriaque, V.; Benali, S.; Moins, S.; Raquez, J.-M.; Gobert, S.; Wattiez, R. Long-term immersion of compostable plastics in marine aquarium: microbial biofilm evolution and polymer degradation. *Mar. Pollut. Bull.* **2023**, *189*, 114711.

(29) Voelker, B. M.; Sedlak, D. L.; Zafiriou, O. C. Chemistry of superoxide radical in seawater: Reactions with organic Cu complexes. *Environ. Sci. Technol.* **2000**, *34* (6), 1036-1042.

(30) Chamas, A.; Moon, H.; Zheng, J.; Qiu, Y.; Tabassum, T.; Jang, J. H.; Abu-Omar, M.; Scott, S. L.; Suh, S. Degradation rates of plastics in the environment. *ACS Sustain. Chem. Eng.* **2020**, *8* (9), 3494-3511.

(31) Maga, D.; Galafton, C.; Blömer, J.; Thonemann, N.; Özdamar, A.; Bertling, J. Methodology to address potential impacts of plastic emissions in life cycle assessment. *Int J Life Cycle Assess* **2022**, *27* (3), 469-491.

(32) R Core Team, R. R: A language and environment for statistical computing. **2021**.

(33) Pischedda, A.; Tosin, M.; Degli-Innocenti, F. Biodegradation of plastics in soil: The effect of temperature. *Polym. Degrad. Stab.* **2019**, *170*, 109017.

(34) Massicotte, P.; South, A.; Hufkens, K. rnaturalearth: World map data from natural earth. *R package version 0.3* **2023**, *2*.

(35) Hijmans, R. J.; Bivand, R.; Forner, K.; Ooms, J.; Pebesma, E.; Sumner, M. D. Package 'terra'. *Maintainer: Vienna, Austria* **2022**.

(36) Hernangómez, D. Using the tidyverse with terra objects: the tidyterra package. *J. Open Source Softw.* **2023**, *8* (91), 5751.

(37) Zhang, L.; Yin, Y.; Sun, Y.; Liang, X.; Graham, D. E.; Pierce, E. M.; Löffler, F. E.; Gu, B. Inhibition of methylmercury and methane formation by nitrous oxide in Arctic tundra soil microcosms. *Environ. Sci. Technol.* **2023**, *57* (14), 5655-5665.

(38) Bolyen, E.; Rideout, J. R.; Dillon, M. R.; Bokulich, N. A.; Abnet, C. C.; Al-Ghalith, G. A.; Alexander, H.; Alm, E. J.; Arumugam, M.; Asnicar, F. Reproducible, interactive, scalable and extensible microbiome data science using QIIME 2. *Nat. Biotechnol* **2019**, *37* (8), 852-857.

(39) Yilmaz, P.; Parfrey, L. W.; Yarza, P.; Gerken, J.; Pruesse, E.; Quast, C.; Schweer, T.; Peplies, J.; Ludwig, W.; Glöckner, F. O. The SILVA and "all-species living tree project (LTP)" taxonomic frameworks. *Nucleic Acids Res.* **2014**, *42* (D1), D643-D648.

(40) Quast, C.; Pruesse, E.; Yilmaz, P.; Gerken, J.; Schweer, T.; Yarza, P.; Peplies, J.; Glöckner, F. O. The SILVA ribosomal RNA gene database project: improved data processing and web-based tools. *Nucleic Acids Res.* **2012**, *41* (D1), D590-D596.

(41) Gómez-Rubio, V. ggplot2-elegant graphics for data analysis. *J. Stat. Softw.* **2017**, *77*, 1-3.

(42) McMurdie, P. J.; Holmes, S. phyloseq: an R package for reproducible interactive analysis and graphics of microbiome census data. *PLoS One* **2013**, *8* (4), e61217.

(43) Oksanen, J.; Blanchet, F. G.; Kindt, R.; Legendre, P.; Minchin, P. R.; O'hara, R.; Simpson, G. L.; Solymos, P.; Stevens, M. H. H.; Wagner, H. Package 'vegan'. *Community ecology package, version* **2013**, *2* (9), 1-295.

(44) Love, M. I.; Huber, W.; Anders, S. Moderated estimation of fold change and dispersion for RNA-seq data with DESeq2. *Genome Biol* **2014**, *15* (12), 1-21.

(45) Wu, G.; Wu, G.; Zhan, T.; Shao, Z.; Liu, Z. Characterization of a cold-adapted and salt-tolerant esterase from a psychrotrophic bacterium *Psychrobacter pacificensis*. *Extremophiles* **2013**, *17*, 809-819.

(46) Zhang, W.; Xu, H.; Wu, Y.; Zeng, J.; Guo, Z.; Wang, L.; Shen, C.; Qiao, D.; Cao, Y. A new cold-adapted, alkali-stable and highly salt-tolerant esterase from *Bacillus licheniformis*. *Int. J. Biol. Macromol.* **2018**, *111*, 1183-1193.

(47) An, T.; Dong, Z.; Lv, J.; Liu, Y.; Wang, M.; Wei, S.; Song, Y.; Zhang, Y.; Deng, S. Purification and characterization of a salt-tolerant cellulase from the mangrove oyster, *Crassostrea rivularis*. *Acta Biochim. Biophys. Sin* **2015**, *47* (4), 299-305.

(48) Voget, S.; Steele, H.; Streit, W. Characterization of a metagenome-derived halotolerant cellulase. *J. Biotechnol.* **2006**, *126* (1), 26-36.

(49) Ferreira, F. V.; Cividanes, L. S.; Gouveia, R. F.; Lona, L. M. An overview on properties and applications of poly (butylene adipate-co-terephthalate)–PBAT based composites. *Polym. Eng. Sci.* **2019**, *59* (s2), E7-E15.

(50) Weng, Y.; Jin, Y.; Meng, Q.; Wang, L.; Zhang, M.; Wang, Y. Biodegradation behavior of poly (butylene adipate-co-terephthalate)(PBAT), poly (lactic acid)(PLA), and their blend under soil conditions. *Polym. Test.* **2013**, *32* (5), 918-926.

(51) Pang, R.; Wang, X.; Zhang, L.; Lei, L.; Han, Z.; Xie, B.; Su, Y. Genome-centric metagenomics insights into the plastisphere-driven natural degradation characteristics and

mechanism of biodegradable plastics in aquatic environments. *Environ. Sci. Technol.* **2024**, *58* (42), 18915-18927.

(52) Wang, G.; Huang, D.; Ji, J.; Völker, C.; Wurm, F. R. Seawater-degradable polymers—fighting the marine plastic pollution. *Adv. Sci* **2021**, *8* (1), 2001121.

(53) Kim, Y.; Choe, S.; Cho, Y.; Moon, H.; Shin, H.; Seo, J.; Myung, J. Biodegradation of poly (butylene adipate terephthalate) and poly (vinyl alcohol) within aquatic pathway. *Sci. Total Environ.* **2024**, *953*, 176129.

(54) Omura, T.; Isobe, N.; Miura, T.; Ishii, S. i.; Mori, M.; Ishitani, Y.; Kimura, S.; Hidaka, K.; Komiyama, K.; Suzuki, M. Microbial decomposition of biodegradable plastics on the deep-sea floor. *Nat. Commun.* **2024**, *15* (1), 568.

(55) Wei, X.-F.; Hedenqvist, M. S. Heatwaves hasten polymer degradation and failure. *Science* **2023**, *381* (6662), 1058-1058.

(56) Samios, E.; Dart, R.; Dawkins, J. Preparation, characterization and biodegradation studies on cellulose acetates with varying degrees of substitution. *Polymer* **1997**, *38* (12), 3045-3054.

(57) Krolicka, A.; Boccadoro, C.; Nilsen, M. M.; Demir-Hilton, E.; Birch, J.; Preston, C.; Scholin, C.; Baussant, T. Identification of microbial key-indicators of oil contamination at sea through tracking of oil biotransformation: An Arctic field and laboratory study. *Sci. Total Environ.* **2019**, *696*, 133715.

(58) Bowman, J. P.; Gosink, J. J.; McCammon, S. A.; Lewis, T. E.; Nichols, D. S.; Nichols, P. D.; Skerratt, J. H.; Staley, J. T.; McMeekin, T. A. *Colwellia demingiae* sp. nov., *Colwellia hornerae* sp. nov., *Colwellia rossensis* sp. nov. and *Colwellia psychrotropica* sp. nov.: psychrophilic Antarctic species with the ability to synthesize docosahexaenoic acid (22: 6 ω 3). *Int. J. Syst. Evol. Microbiol.* **1998**, *48* (4), 1171-1180.

(59) Prabagaran, S. R.; Manorama, R.; Delille, D.; Shivaji, S. Predominance of *Roseobacter*, *Sulfitobacter*, *Glaciecola* and *Psychrobacter* in seawater collected off Ushuaia, Argentina, Sub-Antarctica. *FEMS Microbiol. Ecol.* **2007**, *59* (2), 342-355.

(60) Wang, Y.; Gong, L.; Gao, Z.; Wang, Y.; Zhao, F.; Fu, L.; Li, X. Host-specific bacterial communities associated with six cold-seep sponge species in the South China Sea. *Front Mar Sci* **2023**, *10*, 1243952.

(61) Raggi, L.; García-Guevara, F.; Godoy-Lozano, E. E.; Martínez-Santana, A.; Escobar-Zepeda, A.; Gutierrez-Rios, R. M.; Loza, A.; Merino, E.; Sanchez-Flores, A.; Licea-Navarro, A. Metagenomic profiling and microbial metabolic potential of perdido fold belt (NW) and campeche knolls (SE) in the Gulf of Mexico. *Front Microbiol* **2020**, *11*, 1825.

(62) Hahnke, R. L.; Harder, J. Phylogenetic diversity of *Flavobacteria* isolated from the North Sea on solid media. *Syst Appl Microbiol* **2013**, *36* (7), 497-504.

(63) Yoon, J.; Oku, N.; Matsuda, S.; Kasai, H.; Yokota, A. *Pelagicoccus croceus* sp. nov., a novel marine member of the family *Puniceicoccaceae* within the phylum '*Verrucomicrobia*' isolated from seagrass. *Int. J. Syst. Evol. Microbiol.* **2007**, *57* (12), 2874-2880.

(64) Baek, M.-g.; Shin, S.-K.; Yi, H. *Sphingorhabdus lutea* sp. nov., isolated from sea water. *Int. J. Syst. Evol. Microbiol.* **2019**, *69* (11), 3593-3598.

(65) Degli Innocenti, F.; Breton, T. Intrinsic biodegradability of plastics and ecological risk in the case of leakage. *ACS Sustain. Chem. Eng.* **2020**, *8* (25), 9239-9249.

(66) Lyu; Schley, J.; Loy, B.; Lind, D.; Hobot, C.; Sparer, R.; Untereker, D. Kinetics and time− temperature equivalence of polymer degradation. *Biomacromolecules* **2007**, *8* (7), 2301-2310.